

Application of wavelet analysis in distributed optical fiber Brillouin temperature strain monitoring system

Zhou Feng^{1,2} GanJianjun^{3*} LvHuan² CuiLigang²

¹ Water Conservancy and Civil Engineering Infrastructure Safety Key Laboratory, Nanchang Institute of Technology, Nanchang, China, 330099

² Civil and Architectural Engineering School, Nanchang Institute of Technology, 330099 Nanchang, China

³ School of Water Conservancy and Ecological Engineering, Nanchang Institute of Technology, 330099

E-mail: 251230177@qq.com

Abstract: In the distributed optical fiber monitoring system, the Brillouin system is a system with the most difficult integration, the weakest signal and the most widely used range. It can monitor the strain and temperature of single fiber cable at the same time, and the monitoring range can exceed 100km. It is widely used in super engineering such as submarine optical cable, submarine tunnel, oil pipeline and so on. It is of great research value since this system can monitor the physical quantity of micro deformation, crack and temperature in real time. After the Brillouin system is built independently, the high precision extraction of Brillouin spectrum is realized by using the high efficiency denoising ability of wavelet. By studying the algorithm, the system can reach the temperature identification accuracy of ± 1 degrees centigrade, and the accuracy of strain reaches $\pm 20\mu\varepsilon$.

1. Foreword

The distributed Brillouin optical fiber system can monitor the temperature and strain at the same time by using the Brillouin scattering principle and the BOTDA technology. Such system is distributive, real-time and accurate. Due to the spacial layout of optical fiber, undetection can be avoided. High precision technology can effectively analyze and capture distributed distance information. It is easy to realize automation efficiently and accurately, and the distance of monitoring fiber can even reach hundreds of kilometers. In 2009, Zhao Lijuan^[1] analyzed the key factors affecting the performance of Brillouin system, and proposed a new method to improve the performance of Brillouin system. In 2010, Liu Jianfu^[2] developed the Brillouin monitoring system, which has been applied to practice and achieved good results. In 2011, Huang Min Shuang^[3] et al. Proved that Brillouin system can detect the physical information of the target through the frequency shift of the detected signal. In the same year, Cao Jianmei^[4] designed a Brillouin grid structure system. In 2012, Liu Yangjun^[5] and others analyzed the characteristics of Brillouin signals and proposed the gain of Brillouin signals. With the rapid development of optical fiber sensor system, the monitoring technology of fiber sensor system for civil engineering structures is getting closer to maturity. In 2013, the application of distributed optical fiber sensing technique to the deformation monitoring of No. I landslide in Majiagou, The Three Gorges, was applied by Sun Yijie^[6] and so on. The results showed that the optical fiber sensor system had a



good ability to monitor the abnormal deformation value but lacks an early warning system. In 2014, Lu Yi^[7] used the distributed optical fiber monitoring system to monitor the ground cracks, which made the monitoring space precision to 0.1mm, but the way of storage was fixed-point placement and failed to be stereoscopic.

Wavelet de-noising is a popular denoising method in recent years. It can make up for the lack of signal recognition in the low frequency segment of the traditional denoising method. It can greatly save the response time of the system and play a good de-noising effect. Moreover, wavelet denoising can achieve high resolution requirements. It can control multi-resolution and obtain detailed information in time domain and frequency domain. Therefore, the time windows can be adjusted accordingly for different signals and analysis states. In 1981, Stromberg improved Haar wavelet and established wavelet and wavelet basis functions similar to Haar wavelets. In 1990, Cui Jintai and Wang Jianzhong^[8] used this method to construct a spline wavelet. Because the expression of the wavelet is very clear, it can be used in the process of programming. In 2000, Yuan Changmao, Wen Hongyan^[9] and others used the wavelet denoising method to denoise the deformation monitoring data of buildings and obtained the trend information of buildings. Due to this, the application of wavelet denoising in buildings has become more and more frequent. Based on this, various papers and techniques emerge in endlessly. The two difficult directions of wavelet analysis are the wavelet denoising^[10] and image compression technology^[11]. Combined with the characteristics of wavelet denoising method, this paper adopts wavelet denoising method to reduce Brillouin scattering signal denoising.

2. Experimental Parts

2.1 System Components and Devices

Brillouin system includes system components and test calibration devices. The calibration device includes thermostat and high-precision strain testing device. The temperature range of the thermostat is between room temperature \sim 300 degrees centigrade, the resolution and accuracy are 1 degrees centigrade. The strain gauge accuracy of strain testing device is 20 micro strain. As shown in Figures 1, 2, and 3.

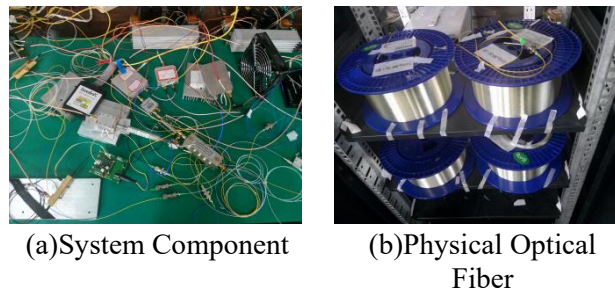


Figure 1 BOTDA System Physical Diagram



Figure 2 Thermostat



(a) (b)
Figure 3 Strain Testing Device

2.2 Testing Methods

The distributed Brillouin optical fiber system is shown in Figure 4. The length of the distributed Brillouin optical fiber system is 15km, the frequency range is from 10550MHz to 10850MHz, the collected data is added 1000 times, the room temperature is 20 degrees centigrade, and at the beginning the fiber is relaxed. A 30m range of optical fiber 10800m is being placed in a constant temperature water bath, and it is heated to 40, 50, 60, 70, 75 and 80 degrees centigrade respectively. Then around 10m range of optical fiber 10830m is being wound round the strain device (Fig. 3), and 500 $\mu\epsilon$, 1500 $\mu\epsilon$, 2500 $\mu\epsilon$, 3500 $\mu\epsilon$ and 4500 $\mu\epsilon$ of strain are applied respectively at room temperature to find out the relationship coefficient of frequency shift with temperature, frequency shift with strain, power with temperature, and power with strain. With the formula of relationship coefficient between temperature and strain with frequency and power obtained through wavelet denoising and traditional fitting method, the temperature and strain of the corresponding position point can be analyzed.

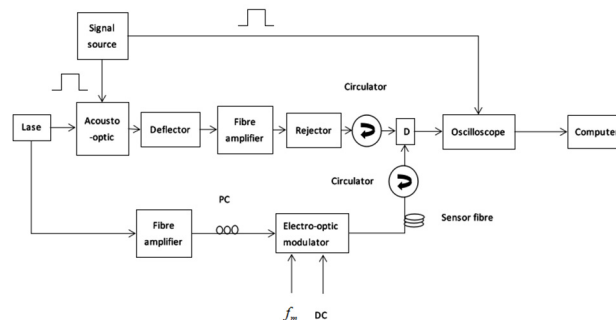


Figure4 BOTDA System Structure Diagram

3. Experiment and Analysis

The data obtained from the Brillouin system at 70 degrees centigrade is shown in Figure 5:

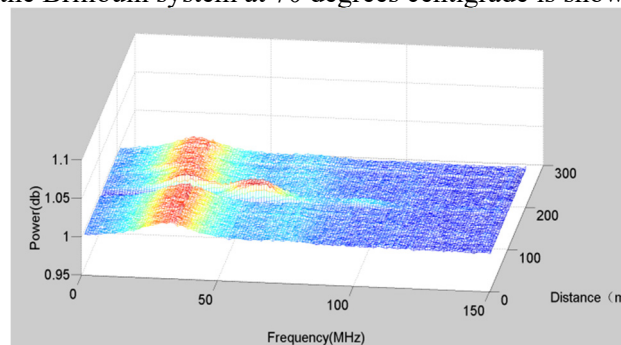


Figure 5 70°C3D Magnification

Figure 6 extracts the scatter plot after the calibration of 1000m position in frequency domain direction,

and combines Lorenz's fitting with scatter plot and Lorenz fitting formula

$$f(x, \theta) = \frac{h(\omega/2)^2}{(x - \nu)^2 + (\omega/2)^2} \quad (1)$$

as shown in Figure 6:

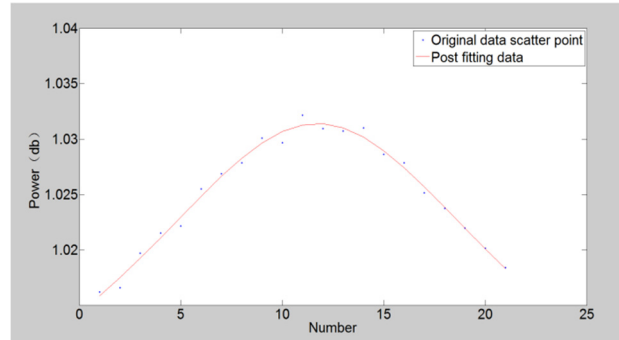


Figure6 Fitting Effect Diagram

The experiment carried out a data processing on threshold denoising in frequency domains respectively under 40, 50, 60, 70 and 80 degrees centigrade, and the data of a total 30m in the range of about 10800 was averaged. Frequency comparison fitted before and after noise reduction is as shown in Table 1:

Table 1 Comparison of Frequency Variation Corresponding to Temperature Change Before and After Filtering

Temperature Value (°C)	Temperature Variation (°C)	Original Data Frequency Value (MHz)	Original Data Frequency Variation Value (MHz)	Frequency Value After Denoising (MHz)	Frequency Variation Value After Denoising (MHz)
20	0	10608	0	10608	0
40	20	10630	22.37	10630	22.32
50	30	10640	31.49	10639	31.39
60	40	10649	40.76	10649	40.60
70	50	10658	50.39	10658	50.25
80	60	10662	54.39	10662	54.16

Power comparison fitted before and after noise reduction is as shown in Table 2:

Table 2 Comparison of Power Variation Corresponding to Temperature Change Before and After Filtering.

Temperature Value (°C)	Temperature Variation (°C)	Original Data Power Value (db)	Original Data Power Variation Value (db)	Power Value After Denoising (db)	Power Variation Value After Denoising (db)
20	0	1.0688	0	1.0687	0
40	20	1.13	0.0612	1.1295	0.0608
50	30	1.1297	0.0609	1.1299	0.0612

60	40	1.13	0.0612	1.1297	0.0610
70	50	1.1309	0.0621	1.1307	0.0620
80	60	1.1314	0.0626	1.1315	0.0628

By conducting linear fitting to the frequency and power after denoising, the relationship coefficient of frequency shift, power and temperature can be obtained. The temperature-frequency shift relationship coefficient were 0.8293 and 0.8236 before and after denoising. By comparing with theoretical value 1.2, we can see that it meets the basic requirement. The temperature-power relationship coefficient is 0.000032 and that after denoising is 0.000048, differ from the theory value 0.000036. This is mainly due to the power difference in fiber optical and regulating light of different manufacturers. Then put the relationship coefficient of the frequency shift, power and temperature into formula 2:

$$\begin{aligned} \Delta_{vb} &= c_1 \Delta_\epsilon + c_2 \Delta_T \\ \frac{100 \Delta P_B}{P_B} &= c_3 \Delta_\epsilon + c_4 \Delta_T \end{aligned} \quad (2)$$

The data obtained under 40°C, 50°C, 60°C, 70°C, 75°C is analyzed, the calculated temperature is filled in Table 3, and the temperature data after denoising is drawn in Figure 7. From Table 3, we could see that the resolution of the temperature after filtering is higher than that of before.

Table 3 Analysis of Temperature Values Before and After Denoising

Theoretical Temperature Value (°C)	Analyzed Temperature Value Before Denoising (°C)	Analyzed Temperature Value After Denoising (°C)
40	44	41.5
50	54	51
60	62.5	61
70	69	70.5
75	76	74.5

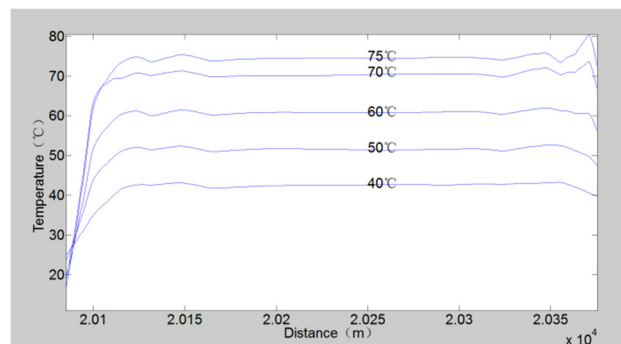


Figure 7 Temperature Curve

By comparison, it can be found that the error range of the analyzed temperature value after denoising is mostly within $\pm 1^\circ\text{C}$, and that of before is far beyond $\pm 1^\circ\text{C}$. Similarly, the data collected under $500 \mu\text{E}$, $1500 \mu\text{E}$, $2500 \mu\text{E}$, and $4500 \mu\text{E}$ is processed in frequency denoising domain, and the data of a total 10m in about 10830 range is averaged. Frequency comparison fitted before and after denoising is as shown in Table 4:

Table 4 Comparison of Frequency Variation Corresponding to Strain Change Before and After Filtering.

Strain Variation ($\mu\epsilon$)	Original Data Frequency Value (MHz)	Original Data Frequency Variation Value (MHz)	Frequency Value After Denoising (MHz)	Frequency Variation Value After Denoising (MHz)
0	10613.07	0	10613.17	0
500	10715.94	102.87	10716.19	103.02
1500	10747.09	134.02	10746.78	133.61
2500	10785.47	172.40	10785.66	172.49
4500	10882.29	269.22	10882.80	269.63

By conducting linear fitting to frequency and power variation after denoising, the relationship coefficient of frequency shift, power and strain can be obtained. The strain-frequency shift relationship coefficient were 0.04209 and 0.04221 before and after denoising. Differ from the theory value 0.048. The main reason is that different manufacturers produce different optical fiber materials, resulting in different degrees of optical loss. The strain-power relationship coefficient is $9.267e-005$, differ greatly from the theory value 0.000036 and this is due to the uneven strain applied by the device thus causing stress concentration at both ends. Therefore, it is necessary to improve the device in later stage. Put the desired relationship coefficient of frequency shift, power and strain into formula 2, then analyze the data collected under $500 \mu\epsilon$ 、 $1500 \mu\epsilon$ 、 $2500 \mu\epsilon$ 、 $3500 \mu\epsilon$ 、 $4500 \mu\epsilon$. The calculated strain values are then being put in Table 5, and the strain data after the denoising is drawn in Figure 8. Through Table 4 we can see that the resolution of strain after filtering is higher than that of before.

Table5 Analysis of Strain Values Before and After Denoising

Theoretical Strain Value ($\mu\epsilon$)	Analyzed Strain Value Before Denoising ($\mu\epsilon$)	Analyzed Strain Value After Denoising ($\mu\epsilon$)
500	556	518
1500	1525	1511
2500	2400	2495
3500	2600	3490
4500	4525	4520

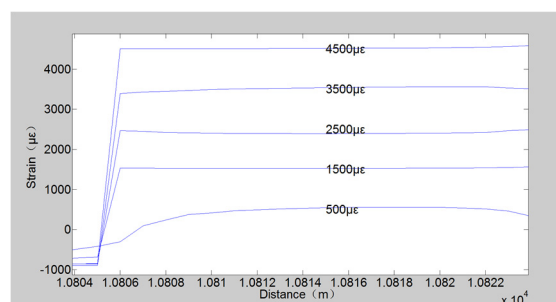


Figure8 Strain Curve

By comparison, it can be found that most of the strain values obtained after denoising are in an error

range of $\pm 20\mu\varepsilon$, and that of before are $\pm 100\mu\varepsilon$. So, the threshold denoising proved to be effective for the measurement of strain.

4. Conclusion

By combining the wavelet threshold denoising algorithm with the traditional curve fitting algorithm, collecting and analyzing the distributed Brillouin optical fiber system based on the BOTDA technology, the following conclusions are drawn:

1) After denoising, the precision of temperature recognition can reach $\pm 1^\circ\text{C}$, and the precision of strain is $\pm 20\mu\varepsilon$. The accuracy of temperature and strain are improved evidently after denoising.

2) After studying the principle of temperature and strain measurement in the distributed Brillouin optical fiber monitoring system and comparing the denoising effect of wavelet group such as sym and DB, it is concluded that the db5 wavelet function is more suitable for the wavelet threshold denoising of this system.

3) The distributed Brillouin optical fiber monitoring software is programmed with the combination of C# language, MATLAB and SQL database. The software realizes data acquisition and analysis to temperature and strain identification.

References

- [1] Zhao Lijuan, Li Yongqian, Zhang Shue, He Yujun. Optical fiber Brillouin scattering spectrum teaching experimental system design [J]. Experimental Technology and Management, 2011, 28 (08): 64-66.
- [2] Li Rongwei, Liu Jianfu, Yang Zhi, Li Yongqian. Research progress of distributed optical fiber temperature and strain sensing technology [J]. Study on Optical Communications, 2010 (03): 44-47.
- [3] Huang Minshuang, Huang Junfen. Optical fiber frequency shift distributed Brillouin optical fiber sensing technology [J]. Acta Photonica Sinica, 2011, 40 (9): 1428-1432.
- [4] Cao Jianmei, Ren Chunnian. Research on deformation monitoring system of optical fiber grid tunnel based on BOTDR [J]. Computer Measurement & Control, 2011, 19 (11): 2616-2618+2628.
- [5] Liu Yangjun, He Julong, Chu Duanduan, XieHongwei. Strain sensitization based on Brillouin sensing technology [J]. Journal of Qinghai University (Natural Science), 2012,30 (04): 26-29.
- [6] Sun Yijie, Zhang Dan, Tong Hengjin and so on. Application of distributed optical fiber monitoring technology in the Majiagou landslide in the Three Gorges Reservoir Area [J]. The Chinese Journal of Geological Hazard and Control, 2013, 24 (4): 97-102.
- [7] Lu Yi, Shi Bin, Xi Jun et al. Research on distributed optical fiber monitoring technology for ground fissure based on BOTDR [J]. Journal of Engineering Geology, 2014, 22 (1): 8-13.
- [8] Huang Daren, Wang Jianzhong. The Budan-Fourier theorem of spline and its application [J]. Chinese Science Bulletin, 1982, 27 (17): 1028-1028.
- [9] Yuan Changmao, Wen Hongyan, YUANChangmao, et al. Wavelet denoising method for deformation monitoring data processing [J]. Geospatial Information, 2009, 7 (4): 136-138.
- [10] Zhang Heng. Simulation and implementation of wavelet denoising technology based on Matlab [J]. Science and Technology of West China, 2010, 09 (29): 4-5.
- [11] Li Zhenwei, He Jishan, Liu Bingquan and so on. Progress in wavelet image compression [J]. Computer Technology and Development, 2004, 14 (6): 29